



# Distributions of environmental radionuclides in a marine core from the eastern continental shelf of Hainan Island, South China Sea and risk assessment

Fengmei Wang<sup>1</sup> · Deming Kong<sup>3</sup> · Liqiang Xu<sup>1,2</sup> · Chao Ji<sup>1</sup> · Lingling Jiang<sup>1</sup>

Received: 19 July 2021 / Accepted: 25 October 2021 / Published online: 8 November 2021  
© Akadémiai Kiadó, Budapest, Hungary 2021

## Abstract

Several long half-life natural and anthropogenic radionuclides, including  $^{137}\text{Cs}$ ,  $^{226}\text{Ra}$ ,  $^{232}\text{Th}$ , and  $^{40}\text{K}$ , in a 45 cm-long sediment core collected from the east continental shelf of Hainan Island, South China Sea, have been analyzed. The results showed that mean activity of  $^{137}\text{Cs}$ ,  $^{226}\text{Ra}$ ,  $^{232}\text{Th}$ , and  $^{40}\text{K}$  were  $2.03 \pm 1.2$ ,  $20.4 \pm 1.8$ ,  $45.7 \pm 3.0$ , and  $520.0 \pm 20.0$  Bq/kg, respectively. Radium equivalent activity and External hazard index imply a low radiation, and the study area could serve as a background reference value for environmental radionuclides in east continental shelf of Hainan Island, South China Sea.

**Keywords** South China Sea · Marine sediments · Radionuclides · Radiological risk assessment

## Introduction

Environmental radionuclides are omnipresent in the Earth environment. Radionuclides with different half-lives may derive from various source materials, making them ideal tools to trace geochemical processes, examine rock ages, and construct the chronology of sediment profiles [1, 2]. However, radionuclides may pose some potential health hazards to human beings through continuous internal and external irradiation [3]. Natural and anthropogenic radionuclides can enter the marine environment through several pathways, such as the discharge of radioactive wastes produced by nuclear tests or nuclear plants, leakage associated with nuclear accidents, weathering and erosion of terrestrial rocks and subsequent transportation by water, wind and gravity, etc., through surface running and groundwater infiltrating. The ocean acts as a sink and reservoir of various terrestrial

materials and marine sediments, which have a high capacity to absorb some radioactive materials [4]. Thus, marine sediments can well record the sedimentary history of radionuclides in the environment [5]. Radionuclides in marine sediments could also play a positive role in chronological analysis, environmental radiological risk assessment, and establishment of environmental radiation safety standards [6–9].

Some areas on the southern coast of China are typical high background radiation areas [10]. In addition, 16 nuclear power plants are currently in regular use in China's coastal areas and more are under construction or proposed for consideration [11]. Terrestrial materials from high radiation background areas and nuclear ore processing by nuclear power plants may release natural and anthropogenic radionuclides [12, 13], which may ultimately enter the ocean.

In addition, based on recent geological survey, continental shelf areas surrounding the Hainan Island were found to be enriched in marine sand resources [14]. These resources are good engineering construction materials with high quality, and future exploitation are under consideration according to the planning of the Chinese government (<https://en.zgss.org.cn/>). The sampling site of this study is located within the planning exploitation area. Thus, radiological risk assessment of these sediments is of great significance. To date, time-series distributions of environmental radionuclides in marine sediments, and their radiological risk in coastal areas are largely unknown. One of our aims is to examine and

✉ Liqiang Xu  
xlq@hfut.edu.cn

<sup>1</sup> School of Resources and Environmental Engineering, Hefei University of Technology, Hefei 230009, Anhui, China

<sup>2</sup> State Key Laboratory of Loess and Quaternary Geology, Institute of Earth Environment, CAS, Xi'an 710061, Shanxi, China

<sup>3</sup> College of Ocean and Meteorology, Guangdong Ocean University, Zhanjiang 524088, Guangdong, China

compare overall radioactivity of the marine sediments in ancient and recent times, respectively.

To assess and monitor the environmental risk of radionuclides, radium equivalent radioactivity ( $Ra_{eq}$ ), which incorporates long half-life radionuclides of  $^{226}\text{Ra}$ ,  $^{232}\text{Th}$  and  $^{40}\text{K}$ , was proposed by scientists [15–19]. It has been widely used to assess radiological risk of marine sediments. For example, Sam et al. [20] analyzed the distributions of natural and man-made radionuclides in the surface sediments of the Sudan and Suakin ports along the Sudan coast of the Red Sea, and identified the influence of organic matter on radionuclide distributions. By analyzing natural radionuclides in the surface sediments of the Vizag coast in southeastern India, Tripathi et al. [21] reported a low level of radioactive hazards. However, soil/beach sand samples in Kalpakkam, India, have much higher levels of long half-life radionuclides, resulting in higher  $Ra_{eq}$  [22]. In addition, a few studies were performed on radionuclides in marine sediments from China. For instance, Liu et al. [23] measured the spatial distributions of radionuclides in the sediments of the Beibu Gulf, South China Sea and reported radioactivities decreasing with the offshore distance. Wang et al. [24] and Lin et al. [25] determined radionuclides in coastal wetlands and marine sediments of the Laizhou Bay, and discussed their potential environmental risks. The external hazard index ( $H_{ex}$ ) is also a good marker for radiological risk [21, 26–28]. In terms of risk assessment of radionuclides in soil or sediments, most of the previous research focused on spatial distribution [29–33], whereas time-series analysis in environmental samples is extremely insufficient.

This study was designed to reconstruct the records of several environmental radionuclides in the sediments of the eastern continental shelf of Hainan Island, South China Sea, and to examine the long-term changes in potential radiological risk. Our study also aids for future management and exploitation of marine sand resources, and helpful for understanding radiological baseline of the study area.

## Materials and methods

### Sample collection

The South China Sea (SCS) is located in the Western Pacific warm pool area and is the largest semi-enclosed marginal sea in the region. It is one of the regions with the highest level of biodiversity in the world [34, 35]. Due to its unique geographical location, the SCS is very sensitive to environmental changes and thus an ideal area for studying global and regional environmental changes [36]. The Pearl River in China and, the Red River, and the Mekong River in Vietnam are the major rivers entering the SCS [34]. These rivers provide the main source materials for


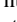
the sediments on the shelf area of the SCS. The study area is located on the eastern continental shelf of Hainan Island, northern SCS.

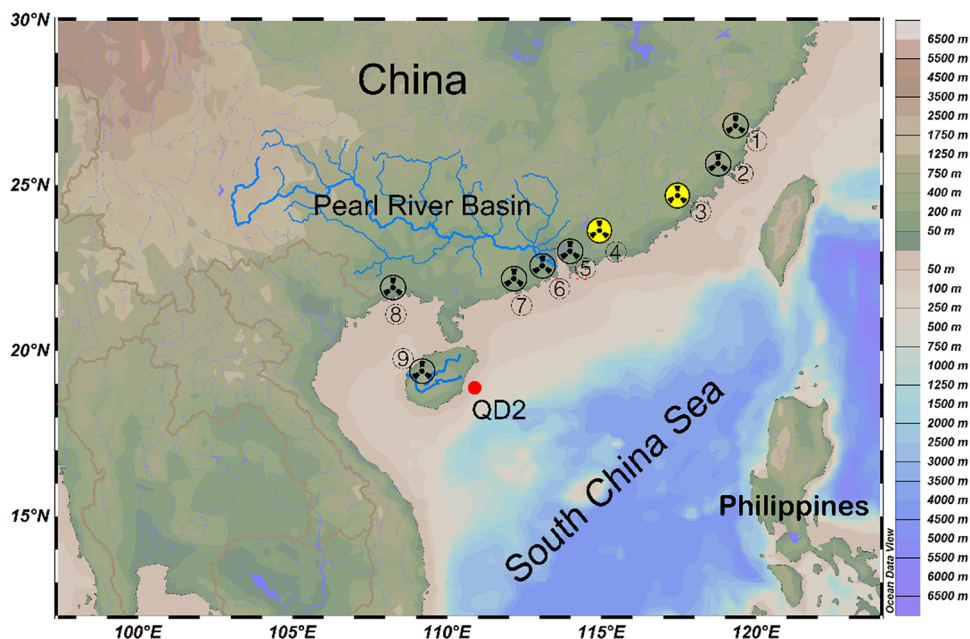
According to previous studies of [37, 38], terrestrial input of the Pearl River is the main sediment source in the northern shelf area of the SCS. Over the past decades, countries around the SCS have been experiencing the fastest economic development with more than 270 million people living in the coastal areas of the SCS. The Pearl River Delta and its city cluster are the most economically developed areas in China, with a large population and high density. To relieve the pressure on energy and resources, the Chinese government has constructed several nuclear power plants on the northern coast of the SCS, and more are under consideration (Fig. 1).

The sediment core analyzed in this study was collected during the “National Natural Science Foundation of China (NSFC) sponsored Open Scientific Expedition Cruise to the western SCS” in 2015 and was named QD2. Though we used one core in the present study, we believe it can generally reflect regional environmental changes. Sediments on the eastern and northern coasts of the South China Sea share a common source, i.e. the Pearl River [37]. The sedimentary environment is thus relatively simple. Similar material sources in this area probably record similar deposition history. Marine productivity record based on QD2 coupled with large scale climatic (temperature, monsoon, etc.) changes [39]. This also partly suggests that the sampling site may serve as a good record for a large area.

The water depth of the sampling site, approximately 20 km offshore, is 84.6 m (coordinates  $18^{\circ}54.00'\text{N}$ ,  $110^{\circ}42.00'\text{E}$ ; Fig. 1). The sampling equipment was supported by vessel “Experiment No. 3” (owned by the South China Sea Institute of Oceanology, Chinese Academy of Sciences). A box corer with a height of 60 cm was used as a sampler. After the sampler was retrieved from the seafloor to the deck, the seawater was siphoned out. A 7.5 cm diameter push core was then inserted into the box corer. The pipe was sealed with made-to-fit ends, and the core was 45 cm in length. Prior to analysis, it was brought back to the laboratory and stored at  $-20^{\circ}\text{C}$ .

The core was opened in the laboratory and sectioned at intervals of 1 cm (45 samples in total). The core was photographed and its lithological characteristics were also recorded in detail. In general, the core could be divided into two parts from the top toward the bottom. The upper part of the core from 0 to 20 cm is composed of yellow–gray fine sand, while sediments at the depth of 20–45 cm are mainly gray–black silt with some tiny mollusk shells [39]. Chronology analysis also revealed that sample age increased with depth (see [Results and discussion](#)), and no evidence of bioturbation was observed during core slicing. We are thus confident that the sediments have been well-preserved and the core serves as a natural archive.

**Fig. 1** Map showing the sampling site and some nuclear power plants (NPPs) on the coast (based on Ocean Data View to create; the red filled circle shows the location of QD2 (which means Qiong-Dong area of the South China Sea); : the running nuclear power units; : NPPs under consideration. The marked numbers in the figure represent the nuclear power plants: ① Ningde NPP; ② Fuqing NPP; ③ Zhangzhou NPP; ④ Taipingleing NPP; ⑤ Daya Bay and Lingao NPP; ⑥ Taishan NPP; ⑦ Yangjiang NPP; ⑧ Fangchenggang NPP; ⑨ Changjiang NPP). (Color figure online)



## Analytical methods

### Chronological and grain size analysis

The age-depth model of the core QD2 was constructed by both  $^{210}\text{Pb}$  analysis of the surface sediments and radiocarbon ( $^{14}\text{C}$ ) dating of foraminifera samples in the lower part sediments. Details of the chronological analysis were described in Ji et al. [39, 40]. Grain size composition of each sample was determined with a laser particle size analyzer after the samples were treated with excess  $\text{H}_2\text{O}_2$  and  $\text{HCl}$ . The analyzer model is Malvern Mastersizer 2000 with a detection range of 0.02–2000  $\mu\text{m}$ .

### Radionuclide analysis

The radionuclides test is specified as follows: after freeze-drying, each sample was ground with an agate mortar and pestle to pass a 100-mesh sieve. Approximately 5–6 g of the sample was transferred to a standard centrifugal tube. The tube was then sealed with cyanoacrylate glue and stored for three weeks to reach the secular radioactive equilibrium between  $^{226}\text{Ra}$  and its daughter isotopes. Sealing is very important for reaching equilibrium between  $^{222}\text{Rn}$  and  $^{226}\text{Ra}$  in the present study. Prior to experiment, we performed leak detection on the tubes we used. A centrifugal tube was sealed with cyanoacrylate glue and then soaked into a 500 mL beaker. No any bubble was observed during this process, implying that leakage of air was impossible. Measurements of the activity concentrations of  $^{137}\text{Cs}$ ,  $^{226}\text{Ra}$ ,  $^{228}\text{Ra}$  and  $^{40}\text{K}$  in Bq/kg (in dry weight) of the collected samples were determined using low-background high-purity germanium

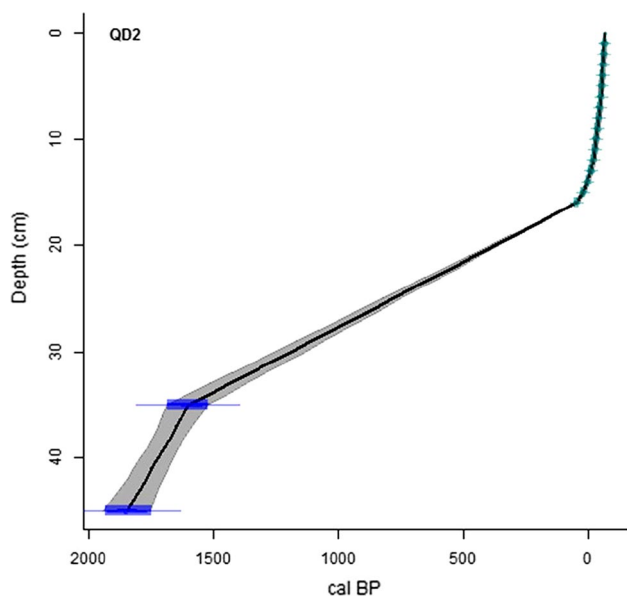
(HPGe) gamma spectrometer. The counter has an energy resolution better than 2.3 keV at 1332 keV (Co-60). Several radionuclides, including  $^{241}\text{Am}$ ,  $^{155}\text{Eu}$ ,  $^{57}\text{Co}$ ,  $^{54}\text{Mn}$ ,  $^{65}\text{Zn}$  and  $^{60}\text{Co}$  (provided by National Institute of Metrology of China), were used to calibrate the spectrometer. The counting time for each sample was approximately 24 h. The detection limit for  $^{137}\text{Cs}$  is 0.19 Bq/kg, and the limit for  $^{226}\text{Ra}/^{228}\text{Ra}/^{40}\text{K}$  is 4.5 Bq/kg.  $^{137}\text{Cs}$  was measured at the position of 661.7 keV. Radioactivity of  $^{226}\text{Ra}$  was obtained by the weighted mean of its daughter isotopes  $^{214}\text{Pb}$  at 295 keV and 351.9 keV and  $^{214}\text{Bi}$  at 609.3 keV. For  $^{228}\text{Ra}$  measurement, the weighted mean was taken from signals at the 338.3 keV, 911.2 keV, and 968.8 keV peaks of  $^{228}\text{Ac}$ . The photopeak for  $^{40}\text{K}$  was 1460.8 keV.

## Results and discussion

### Chronology and grain size compositions

According to the age-depth model constructed for QD2 by  $^{210}\text{Pb}$  and  $^{14}\text{C}$  tests, the ages of the QD2 samples increase with the depth without age inversion, implying good preservation of the samples. The age of the bottom sample of this core is 1852 years before present (106 AD), suggesting the core has a history of approximately 1900 years [39, 40] (Fig. 2).

Grain size compositions of sediment samples in QD2 were provided in Fig. 3. It tells that the sediments mainly consist of coarse components, i.e. sand and silt. In contrast, the content of clay is low. Additionally, the concentrations of typical land-origin element Aluminum (Al)

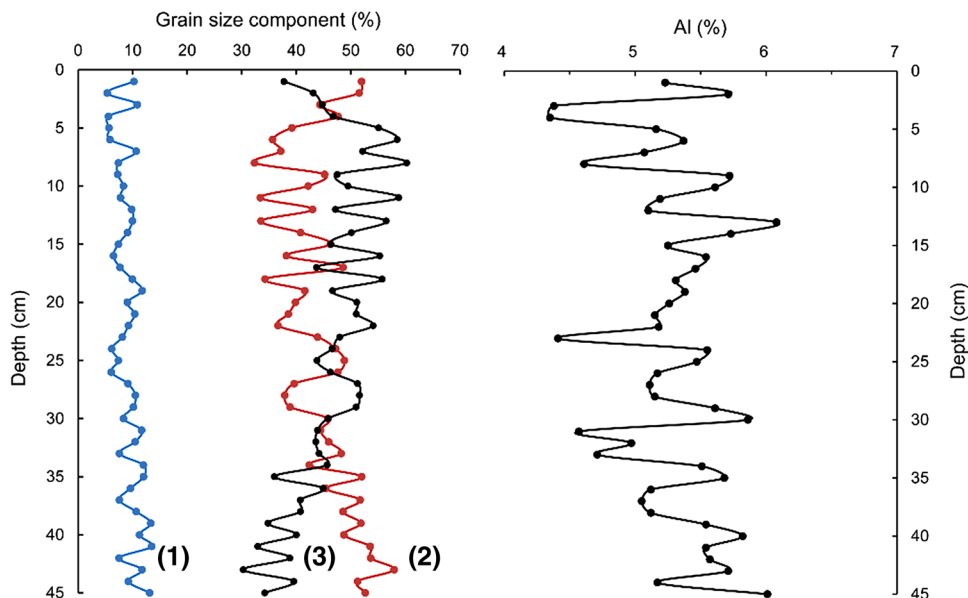


**Fig. 2** Age-depth model for the profile QD2 based on  $^{210}\text{Pb}$  and  $^{14}\text{C}$  dating (Reprinted from [40] with permission from Wiley)

in this core are as high as ~4–6% [39]. This implies terrestrial input is the dominant source of these sediments. This is in agreement with an earlier study which reported that sediments from this study area were derived from the Pearl River [37].

Based on statistics, both sand and silt have relatively small coefficients of variation (CV) (~15%). Together with the relatively uniform lithology, the results suggest that the sediments in the study site could be in a relatively stable sedimentary environment, and the source material has not changed significantly.

**Fig. 3** Down core distributions of grain components [(1) clay, (2) silt and (3) sand] and Al (the data of Al are cited from reference [39])



### Distribution of nuclides in the sedimentary profile

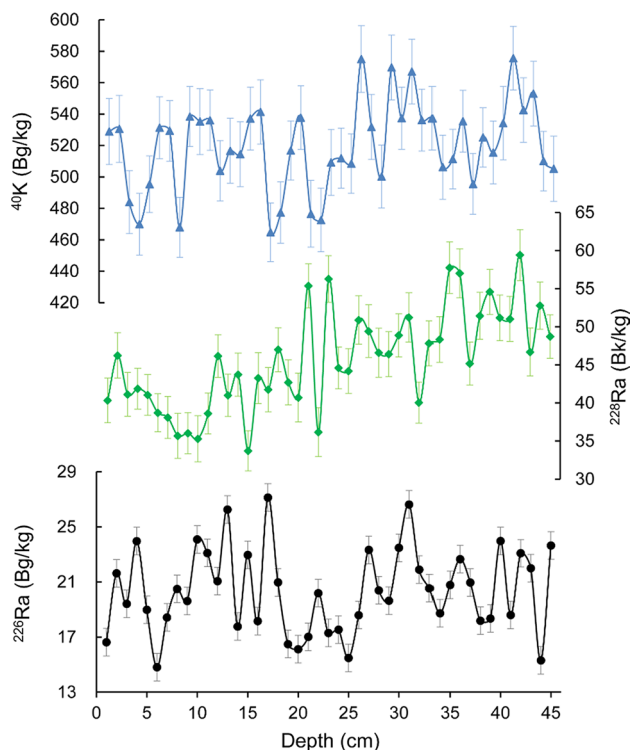
Among the radionuclides that we analyzed,  $^{137}\text{Cs}$  has the lowest radioactivity. It was found in the sediments above depth of 5 cm, and the radioactivity concentrations for these five samples are 4.0, 2.2, 1.8, 0.7, and 1.4 Bq/kg, respectively. The  $^{137}\text{Cs}$  signal in the upper most layer could be a record of Fukushima Daiichi nuclear disaster in 2011.  $^{137}\text{Cs}$  shows a small peak at the depth of 5 cm, and this might be measured from the Chernobyl nuclear accident. The distribution of  $^{137}\text{Cs}$  in core QD2 also suggests a relatively low sedimentation rate. The missing of  $^{137}\text{Cs}$  in deep layers could be explained by its natural decay, as it has a relatively “short” half-life in comparison with  $^{226}\text{Ra}$ ,  $^{228}\text{Ra}$  and  $^{40}\text{K}$ . The anthropogenic  $^{137}\text{Cs}$  data also imply an insignificant impact of human activity on the sediments.

The activity concentrations of long-lived natural radionuclides  $^{226}\text{Ra}$ ,  $^{228}\text{Ra}$ , and  $^{40}\text{K}$  in QD2 sediment core are given in Fig. 4.

Figure 4 shows that the radioactivity of  $^{226}\text{Ra}$  in QD2 ranges from 14.8 to 27.1 Bq/kg with an average of  $20.4 \pm 1.8$  Bq/kg ( $n=45$ ). The minimum value appears at the depth of 6 cm and the maximum appears at 17 cm. The radioactivity of  $^{226}\text{Ra}$  between 18 and 30 cm is slightly lower, but its overall trend is not evident.

The radioactivity of  $^{226}\text{Ra}$  in QD2 is slightly lower than the worldwide average concentration of 35 Bq/kg [41] and significantly lower than most of the reported radioactivities of soil and sediment samples in China (Table 1). For example,  $^{226}\text{Ra}$  radioactivities in soil samples of the Pearl River Delta and surface sediments from Nansha are as high as 135.9 Bq/kg and 80.6 Bq/kg, respectively [42, 43]. The Huangmao Sea-Guanghai Bay and adjacent sea areas and





**Fig. 4** Radioactivity-versus-depth profiles of  $^{226}\text{Ra}$ ,  $^{228}\text{Ra}$ , and  $^{40}\text{K}$  in QD2 core with depth

the Yangjiang nuclear power sea area also have much higher activity concentrations of  $^{226}\text{Ra}$  [10, 44]. This large variability of  $^{226}\text{Ra}$  could be partly attributed to the type of soil/sediments, soil parent material, landform and radiochemistry in specific areas. For instance, the Pearl River Delta watershed is an area with high radiation background [45, 46], leading to a relatively high level of  $^{226}\text{Ra}$  in its soil sediments. In terms of the absolute values, the radioactivity of  $^{226}\text{Ra}$  in QD2 is approximately half of the average radioactivity of  $^{226}\text{Ra}$  in Chinese soil, i.e. 37.6 Bq/kg [47].

Compared to  $^{226}\text{Ra}$ ,  $^{228}\text{Ra}$  in the QD2 sediments has higher radioactivity ranging from the minimum of 33.7 Bq/kg (at 15 cm) to the maximum of 59.4 Bq/kg (at 42 cm), with an average of  $45.7 \pm 3.0$  Bq/kg ( $n=45$ ). Throughout the entire profile, the radioactivity of  $^{228}\text{Ra}$  in the upper part (0–20 cm) of the core is lower than that of the lower sediments (Fig. 4). From a global perspective, the  $^{228}\text{Ra}$  radioactivities in the QD2 core are higher than the international average of 30 Bq/kg [41].

Among the analyzed radionuclides,  $^{40}\text{K}$  in QD2 core shows relatively higher radioactivity level (Fig. 4) between 464.8 and 575.6 Bq/kg, with an average of  $520.0 \pm 20.0$  Bq/kg. The radioactivity of  $^{40}\text{K}$  in QD2 core was higher than those in some previously investigated coastal areas of China, e.g. the Beibu Gulf, Bailong Peninsula, Pearl River Estuary and Nansha sea area (253–511.5 Bq/kg) [48–52]. Conversely, the radioactivity of  $^{40}\text{K}$  in QD2 core was overall

**Table 1** The  $\text{Ra}_{\text{eq}}$  values in marine and estuary sediments

Area	Radioactivity (Bq/kg)			$\text{Ra}_{\text{eq}}$ (Bq/kg)	References
	$^{226}\text{Ra}$	$^{228}\text{Ra}$	$^{40}\text{K}$		
South China Sea Coral Reef	3.3	5.1	24.4	12.5	[25]
Beibu Gulf*	22.2	34.4	253.0	90.9	[48]
Pearl River Estuary, Dapeng Bay and Daya Bay	27.9	36.5	456.2	115.2	[50]
Shenzhen coastal areas	26.5	43.2	364.2	116.3	[51]
The adjacent areas to Bailong Peninsula, Beibu Gulf*	32.4	46.1	355.0	125.7	[49]
Continental shelf areas of Hainan Island	20.4	45.7	520.0	125.7	This study
Yangtze River Estuary	24.3	40.9	628.0	131.1	[71]
Northeast of South China Sea	27.7	44.9	538.0	133.3	[23]
Yangtze River Estuary and adjacent areas*	18.5	48.5	684.0	140.5	[72]
Hong Kong sea areas	32.5	48.1	625.0	149.4	[73]
Changyi Coastal Wetland/Laizhou Bay	28.6	57.9	542.0	153.1	[15]
Tianwan Sea Area, Lianyungang	25.2	46.7	899.0	161.2	[56]
Jiaozhou Bay	26.5	40.3	688.0	164.4	[53, 74]
Yangjiang Nuclear Power Sea Area	35.5	57.1	621.0	165.0	[10]
Huangmao Sea-Guanghai Bay and adjacent sea areas	36.6	61.3	571.0	168.2	[44]
Xinghua Bay, Fujian	24.8	63.7	734.0	172.4	[55]
Intertidal zone in Xiamen sea areas	32.4	69.3	692.0	184.8	[54]
Nansha sea area	80.6	45.5	511.5	185.0	[52]
Pearl River Delta	135.9	196.9	670.2	469.1	[42]

$\text{Ra}_{\text{eq}}$  values in areas marked with asterisks were given in the cited papers.  $\text{Ra}_{\text{eq}}$  in areas without asterisks were calculated by nuclide activity values provided in the respective paper(s)

lower than those in sediments from the northeastern of SCS, Laizhou Bay, Xinghua Bay, Taiwan sea and other investigated areas (538–899 Bq/kg) [10, 43, 53–56]. In general, the average radioactivity of  $^{40}\text{K}$  in QD2 core is slightly lower than the average radioactivity of  $^{40}\text{K}$  in China (584.0 Bq/kg), but higher than the global average of 400 Bq/kg. To further assess the overall long-term environmental risk of radionuclides in the study area, we calculated the  $\text{Ra}_{\text{eq}}$  index based on the measured radioactivity concentrations of  $^{226}\text{Ra}$ ,  $^{228}\text{Ra}$  and  $^{40}\text{K}$ .

### Radiological risk assessment of radionuclides in core QD2

Individual radionuclides may not reflect the overall long-term risk of the bulk sediments, and an integrated marker is thus required. Hazard indexes could be good indicators that reflect general radioactivity of environment samples. Such indexes are thus employed to investigate changes in radiation of marine sediments on millennial scales. The utilization of hazard indexes to examine marine sediments was generally acknowledged by scientific community, and the indexes have been applied to some ocean areas, including the Bay of Algeiras [57], shore of Vizag [21] and the southern South China Sea [58]. As stated above, the core dates back approximately 1900 years. Together with the established chronology, we used radium equivalent activity and external hazard index to evaluate radiological risk over the last ~1900 years.

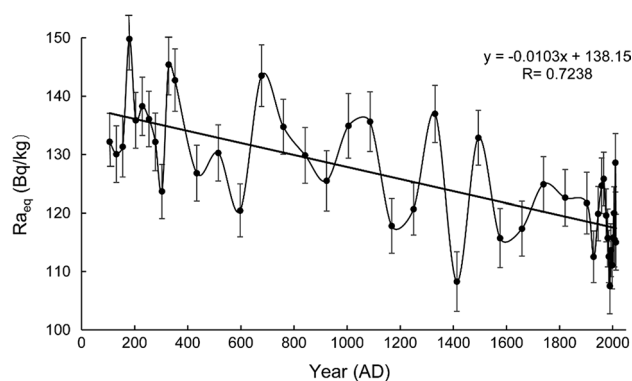
#### Radium equivalent activity ( $\text{Ra}_{\text{eq}}$ )

In order to compare the comprehensive radiological effects of the main natural radionuclides in the continental shelf of eastern Hainan Island,  $\text{Ra}_{\text{eq}}$  was used to evaluate the radioactivity of each sample in QD2 sediment core, which is widely used in radioactive risk assessment [59–61]. The hazard index is calculated based on the activity of natural long half-life radionuclides  $^{226}\text{Ra}$ ,  $^{232}\text{Th}$  and  $^{40}\text{K}$ , mathematically defined as follows [62–65]:

$$\text{Ra}_{\text{eq}} = A_{\text{Ra}} + 1.43 \times A_{\text{Th}} + 0.077 \times A_{\text{K}} \quad (1)$$

where  $A_{\text{Ra}}$ ,  $A_{\text{Th}}$ ,  $A_{\text{K}}$  are the activity concentrations of  $^{226}\text{Ra}$ ,  $^{232}\text{Th}$ , and  $^{40}\text{K}$  in the sediments, respectively. It is generally accepted that the radioactivity of  $^{232}\text{Th}$  is equal to its decay daughter  $^{228}\text{Ra}$  due to secular equilibrium [26, 28, 63, 66]. Thus,  $^{228}\text{Ra}$  is frequently used as a substitution for  $^{232}\text{Th}$  in the calculation of  $\text{Ra}_{\text{eq}}$ . Based on chronology and activity data, we have constructed a 1900-year record of  $\text{Ra}_{\text{eq}}$  for the QD2 core (Fig. 5), which is the first long-term, i.e. millennial-scale,  $\text{Ra}_{\text{eq}}$  record.

Figure 5 shows the minimum value of  $\text{Ra}_{\text{eq}}$  is 107.5 Bq/kg at the year of 1989 AD, and the maximum (149.8 Bq/kg)



**Fig. 5**  $\text{Ra}_{\text{eq}}$  values for sediments in the core QD2 over the past 1900 years

kg) appears at 180 AD. The present-day  $\text{Ra}_{\text{eq}}$  of 115.0 Bq/kg is approximately 77% of the maximum. The average  $\text{Ra}_{\text{eq}}$  over the past 1900 years is  $125.7 \text{ Bq/kg} \pm 10.4$  ( $n=45$ ). In general,  $\text{Ra}_{\text{eq}}$  of 370 Bq/kg is widely accepted by the scientific community as a safety threshold [34, 67–70]. In comparison with this recommendation value, the  $\text{Ra}_{\text{eq}}$  of sediments from the eastern continental shelf of the Hainan Island, SCS, is significantly lower. This suggests that the radiological hazard in the study area is low. It is also noted that  $\text{Ra}_{\text{eq}}$  shows a decreasing trend in the past 1900 years (Fig. 5) and is currently at a relatively low level, which is only 31% of the safety threshold.

We compared the  $\text{Ra}_{\text{eq}}$  values of marine and estuary sediments in some other areas of China by compiling the published  $\text{Ra}_{\text{eq}}$  data (Table 1). According to this table, sediment  $\text{Ra}_{\text{eq}}$  values in other regions of China are generally low, ranging from 12.5 to 469.0 Bq/kg. The overall radioactivity level of the QD2 samples is similar to that of marine sediments in some coastal areas of China (such as the sediments adjacent to the Bailong Peninsula in Beibu Gulf and the surface sediments in the Yangtze River estuary) but lower than the average radioactivity of the Chinese soils (165.7 Bq/kg)[42].

Due to the widespread granite and acidic volcanic rocks around the Pearl River Delta, northern coast of the South China Sea is a high radiation background area and geological samples there contain high levels of uranium and thorium, and its  $\text{Ra}_{\text{eq}}$  (469.1 Bq/kg) exceeds the safety threshold of 370 Bq/kg (Table 1) [10, 42, 73, 74]. All the other investigated areas in China, including the coast area in this study, have  $\text{Ra}_{\text{eq}}$  values below the threshold, further attesting to a low radiological risk. Therefore, the  $\text{Ra}_{\text{eq}}$  data obtained in this study can serve as the background value of radioactivity in the study area. The average value can be further used as an environmental background to guide environmental management and decision-making concerning environmental radioactivity.

We also investigated the radioactivities of radionuclides in samples around the globe.  $Ra_{eq}$  data from different regions of the world are presented in Fig. 6 [47, 75–78]. Figure 6 shows most studies on soil/sediment radioactivity are from Europe [20, 41, 79], East Asia and South Asia [22, 56, 74, 80], with a few related studies from West Asia [81–83]. Comparatively, studies of  $Ra_{eq}$  from Africa, Australia and America are scarce [26, 84, 85].

The average radioactivity of QD2 samples is (125.7 Bq/kg) slightly higher than that of the world average of 108.7 Bq/kg [41]. Available global data show the radioactivities of sediments and soils from Europe are relatively low [41, 79]. The European average  $Ra_{eq}$  value is very close to that of QD2 samples in this study (125.7 Bq/kg), and the lowest radioactivity (43.1 Bq/kg) is from the Black Sea coast of Turkey [86]. Among all the data we collected, the maximum  $Ra_{eq}$  is from Kalpakkam, India [22], which is as high as 644.1 Bq/kg, about four times greater than sediments in our study. From a global perspective, the average radioactivity level in sediments from the eastern continental shelf of Hainan Island, SCS, is at a medium level and below the safety threshold. Therefore, the study area is at low radiological risk.

#### External hazard index ( $H_{ex}$ )

The external hazard index ( $H_{ex}$ ) is also a good indicator of radiological risk. The sediments in the marine environment mainly come from the nearby land continent. Thus,  $H_{ex}$  can be used to estimate the hazard of natural gamma radiation

of the marine sediments and the terrestrial mainland [21, 58, 87]. The calculation formula is as follows [21]:

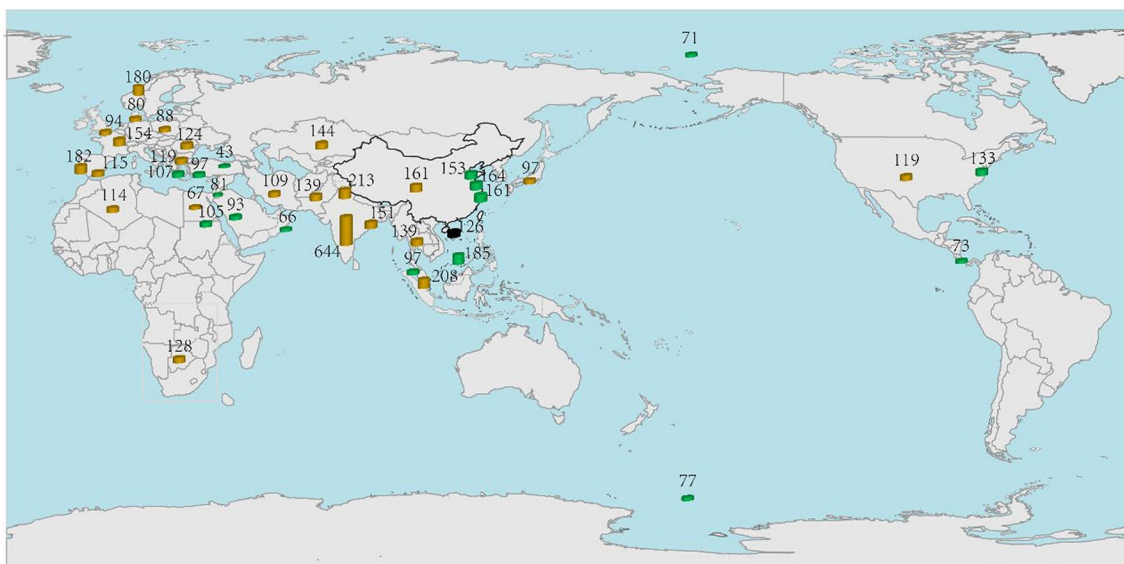
$$H_{ex} = A_{Ra}/370 + A_{Th}/259 + A_K/4810 \quad (2)$$

The results revealed that  $H_{ex}$  values of QD2 core samples ranged from 0.29 to 0.40, with an average of 0.34, less than the safety threshold value 1 [26, 65, 88, 89]. In comparison with published some  $H_{ex}$  values of marine sediments (e.g. Southeast India, Egyptian Red Sea Coast, Southern Italy and Upper Gulf of Thailand etc.), our values are low. This also suggests that the risk of external radiation hazards is very small.

Based on  $Ra_{eq}$  and  $H_{ex}$ , together with the pretty low level of  $^{137}Cs$ , it is concluded that the delivery of land-based materials to the sediments and nuclear power plant operations (including nuclear ore processing) nowadays in China's coastal areas do not cause great radiation hazards.

## Conclusions

A sediment core QD2 was collected from the eastern continental shelf of Hainan Island, SCS. Several radionuclides, including  $^{137}Cs$ ,  $^{226}Ra$ ,  $^{228}Ra$  and  $^{40}K$  were determined. The activities of  $^{137}Cs$  are very low, suggesting a minor impact of anthropogenic impact. Average activities of  $^{226}Ra$ ,  $^{228}Ra$  and  $^{40}K$  are  $20.4 \pm 1.8$  Bg/kg,  $45.7 \pm 3.0$  Bg/kg, and  $520.0 \pm 20.0$  Bq/kg. In combination with chronological analysis, the time-series distributions of  $^{226}Ra$ ,  $^{228}Ra$ ,  $^{40}K$  in the sediments of the core were reconstructed. Radium



**Fig. 6** Global distributions of soil/sediment  $Ra_{eq}$  values (black bar denotes marine sediments in this study; green and yellow markers represent sediment and soil samples, respectively). (Color figure online)

equivalent activity ( $R_{a_{eq}}$ ) and external hazard index ( $H_{ex}$ ) were employed to evaluate the radiation risk. The mean value of  $R_{a_{eq}}$  and  $H_{ex}$  are 125.7 Bq/kg and 0.34, respectively. The  $R_{a_{eq}}$  value of QD2 is generally low with an average of 125.7 Bq/kg, much smaller than the  $R_{a_{eq}}$  safety threshold (370 Bq/kg). Thus, the environmental risk associated with radionuclides around the study area should be low. In combination with chronological analysis, a 1900-year record of  $R_{a_{eq}}$  was reconstructed, and the record shows a decreasing trend in  $R_{a_{eq}}$ .  $H_{ex}$  average is less than the safety threshold 1. Both  $R_{a_{eq}}$  and  $H_{ex}$  suggest a low radiological risk. Together with low level of  $^{137}\text{Cs}$ , it is concluded that the environmental risk associated with radionuclides around the study area should be low. The eastern continental shelf area of Hainan Island, SCS, could serve as a natural background in environmental radiation studies. The results of this study provide reference values for the assessment of marine radiation safety in coastal areas and monitoring of radionuclide pollution.

**Acknowledgements** This work was financially supported by the Fundamental Research Funds for the Central Universities (PA2021KCPY0047), the open research fund of the State Key Laboratory of Loess and Quaternary Geology, Institute of Earth Environment, Chinese Academy of Sciences (SKLLQG1929), and National Natural Science Foundation of China (41606070). Jianguo Liu and other team members helped sampling. Raw data for this study is available at public repository Zenodo: <https://doi.org/10.5281/zenodo.5112050>.

**Author contribution** All authors contributed to the study conception and design. Material preparation, data collection and analysis were performed by Fengmei Wang, Chao Ji and Lingling Jiang. The first draft of the manuscript was written by Fengmei Wang and all authors commented on previous versions of the manuscript. All authors read and approved the final manuscript.

## Declarations

**Conflict of interest** The authors have no conflicts of interest to declare that are relevant to the content of this article.

## References

- Lin WH, Yu KF, Wang YH, Liu XM, Chen LQ (2020) Using uranium-series radionuclides as tools for tracing marine sedimentary processes: source identification, sedimentation rate, and sediment resuspension. *Mar Geol Quat Geol* 40(01):60–70
- Steinhauser G (2014) Fukushima's forgotten radionuclides: a review of the understudied radioactive emissions. *Environ Sci Technol* 48(9):4649–4663. <https://doi.org/10.1021/es405654c>
- Wang JL, Du JZ, Bi QQ (2017) Natural radioactivity assessment of surface sediments in the Yangtze Estuary. *Mar Pollut Bull* 114(1):602–608. <https://doi.org/10.1016/j.marpolbul.2016.09.040>
- LI H (2009) Investigation and research on radionuclides in Qingdao offshore M.D. Dissertation, Ocean University of China
- Akram M, Qureshi RM, Ahmad N, Solaija TJ (2006) Gamma-emitting radionuclides in the shallow marine sediments off the Sindh coast, Arabian Sea. *Radiat Prot Dosim* 118(4):440–447. <https://doi.org/10.1093/rpd/nci355>
- Huang DK, Du JZ, Zhang J (2011) Particle dynamics of  $^7\text{Be}$ ,  $^{210}\text{Pb}$  and the implications of sedimentation of heavy metals in the Wenjiao/Wenchang and Wanquan River estuaries, Hainan, China. *Estuar Coast Shelf Sci* 93(4):431–437. <https://doi.org/10.1016/j.ecss.2011.05.013>
- Wang JL, Du JZ, Baskaran M, Zhang J (2016) Mobile mud dynamics in the East China Sea elucidated using  $^{210}\text{Pb}$ ,  $^{137}\text{Cs}$ ,  $^7\text{Be}$ , and  $^{234}\text{Th}$  as tracers. *J Geophys Res Oceans* 121(1):224–239. <https://doi.org/10.1002/2015jc011300>
- Huang DK, Du JZ, Deng B, Zhang J (2013) Distribution patterns of particle-reactive radionuclides in sediments off eastern Hainan Island, China: implications for source and transport pathways. *Cont Shelf Res* 57:10–17. <https://doi.org/10.1016/j.csr.2012.04.019>
- Seddeek MK, Badran HM, Sharshar T, Elnimr T (2005) Characteristics, spatial distribution and vertical profile of gamma-ray emitting radionuclides in the coastal environment of North Sinai. *J Environ Radioact* 84(1):21–50. <https://doi.org/10.1016/j.jenvrad.2005.03.005>
- Wu MG, Zhou P, Zhao F, Li DM, Zhao L, Zheng YL, Cai WX, Fang HD, Lou QS (2018) The concentration of  $\gamma$  radionuclides in surface marine sediments from Yangjiang nuclear power plant and its adjacent sea area, South China Sea. *Mar Environ Sci* 37(01):43–47. <https://doi.org/10.13634/j.cnki.mes.2018.01.008>
- National nuclear safety administration (2021) Overall safety state of nuclear power plants in China. <http://spi.mee.gov.cn:8080/spi/>
- Ballová S, Pipík M, Friták V, Soja G (2020) Pyrogenic carbon for decontamination of low-level radioactive effluents: Simultaneous separation of  $^{137}\text{Cs}$  and  $^{60}\text{Co}$ . *Prog Nucl Energy* 129:103484. <https://doi.org/10.1016/j.pnucene.2020.103484>
- Bondar'kov MD, Maksimenko AM, Vishnevskii IN, Zheltonozhskii MV, Zheltonozhskaya MV, Boyarishchev VV (2009) Radioactivity in technological NPP waste. *Bull Russ Acad Sci Phys* 73(2):266–269. <https://doi.org/10.3103/S1062873809020312>
- Tong CL, Sun LF, Huang SR (2020) Main progress and achievements of marine geological survey in Hainan Province. *Geol Surv China* 007(001):60–70. <https://doi.org/10.19388/j.zgdzdc.2020.01.09>
- Wang QD, Song JM, Li XG, Yuan HM, Li N, Cao L (2016) Distribution and environmental significances of radionuclides in the sediment of the Changyi Coastal Wetland. *Environ Sci* 37(08):3026–3033. <https://doi.org/10.13277/j.hjxx.2016.08.025>
- Veiga R, Sanches N, Anjos RM, Macario K, Bastos J, Iguatemy M, Aguiar JG, Santos AMA, Mosquera B, Carvalho C, Baptista Filho M, Umisedo NK (2006) Measurement of natural radioactivity in Brazilian beach sands. *Radiat Meas* 41(2):189–196. <https://doi.org/10.1016/j.radmeas.2005.05.001>
- Örgün Y, Altınsoy N, Şahin SY (2007) Natural and anthropogenic radionuclides in rocks and beach sands from Ezine region (Çanak-kale), Western Anatolia, Turkey. *Appl Radiat Isot* 65(6):739–747. <https://doi.org/10.1016/j.apradiso.2006.06.011>
- Al-Hamarneh IF, Awadallah MI (2009) Soil radioactivity levels and radiation hazard assessment in the highlands of northern Jordan. *Radiat Meas* 44(1):102–110. <https://doi.org/10.1016/j.radmeas.2008.11.005>
- Calin MR, Radulescu I, Ion AC, Capra L, Almasan ER (2020) Investigations on chemical composition and natural radioactivity levels from salt water and peloid used in pelotherapy from the Techirghiol Lake, Romania. *Environ Geochem Health* 42(3):513–529. <https://doi.org/10.1007/s10653-019-00382-8>
- Sam AK, Elganawi AA, Ahamed MMO, ElKhanghi FA (1998) Distribution of some natural and anthropogenic radionuclides in Sudanese harbour sediments. *J Radioanal Nucl Chem* 237(1):103–107. <https://doi.org/10.1007/BF02386670>



21. Tripathi RM, Patra AC, Mohapatra S, Sahoo SK, Kumar AV, Puranik VD (2012) Natural radioactivity in surface marine sediments near the shore of Vizag, South East India and associated radiological risk. *J Radioanal Nucl Chem* 295(3):1829–1835. <https://doi.org/10.1007/s10967-012-2106-2>
22. Kannan V, Rajan MP, Iyengar MAR, Ramesh R (2002) Distribution of natural and anthropogenic radionuclides in soil and beach sand samples of Kalpakkam (India) using hyper pure germanium (HPGe) gamma ray spectrometry. *Appl Radiat Isot* 57(1):109–119. [https://doi.org/10.1016/S0969-8043\(01\)00262-7](https://doi.org/10.1016/S0969-8043(01)00262-7)
23. Liu GS, Huang YP, Chen M, Qiu YS, Cai YH, Gao ZY (2001) Specific activity and distribution of natural radionuclides and  $^{137}\text{Cs}$  in surface sediments of the northeastern South China Sea. *Acta Oceanol Sin* 06:76–84
24. Wang QD, Song JM, Li XG, Yuan HM, Li N, Cao L (2015) Environmental radionuclides in a coastal wetland of the Southern Laizhou Bay, China. *Mar Pollut Bull* 97(1):506–511. <https://doi.org/10.1016/j.marpolbul.2015.05.035>
25. Lin WH, Yu KF, Wang YH, Liu XM, Ning QY, Huang XY (2019) Radioactive level of coral reefs in the South China Sea. *Mar Pollut Bull* 142:43–53. <https://doi.org/10.1016/j.marpolbul.2019.03.030>
26. El-TaHER A, Madkour HA (2011) Distribution and environmental impacts of metals and natural radionuclides in marine sediments in-front of different wadies mouth along the Egyptian Red Sea Coast. *Appl Radiat Isot* 69(2):550–558. <https://doi.org/10.1016/j.apradiso.2010.11.010>
27. Khuntong S, Phaophang C, Sudprasert W (2015) Assessment of radionuclides and heavy metals in marine sediments along the Upper Gulf of Thailand. *J Phys Conf Ser* 611:012023
28. Caridi F, Messina M, Faggio G, Santangelo S, Messina G, Belmusto G (2018) Radioactivity, radiological risk and metal pollution assessment in marine sediments from Calabrian selected areas, southern Italy. *Eur Phys J Plus* 133(2):65. <https://doi.org/10.1140/epjp/i2018-11887-1>
29. Singh J, Singh H, Singh S, Bajwa BS, Sonkawade RG (2009) Comparative study of natural radioactivity levels in soil samples from the Upper Siwaliks and Punjab, India using gamma-ray spectrometry. *J Environ Radioact* 100(1):94–98. <https://doi.org/10.1016/j.jenvrad.2008.09.011>
30. Godoy JM, Schuch LA, Nordemann DJR, Reis VRG, Ramalho M, Recio JC, Brito RRA, Olech MA (1998)  $^{137}\text{Cs}$ ,  $^{226}\text{Ra}$ ,  $^{210}\text{Pb}$  and  $^{40}\text{K}$  concentrations in Antarctic soil, sediment and selected moss and lichen samples. *J Environ Radioact* 41(1):33–45. [https://doi.org/10.1016/S0265-931X\(97\)00084-2](https://doi.org/10.1016/S0265-931X(97)00084-2)
31. Ababneh ZQ, Al-Omari H, Rasheed M, Al-Najjar T, Ababneh AM (2010) Assessment of gamma-emitting radionuclides in sediment cores from the Gulf of Aqaba, Red Sea. *Radiat Prot Dosim* 141(3):289–298. <https://doi.org/10.1093/rpd/ncq182>
32. Muhammad BG, Jaafar MS, Rahman AA, Ingawa FA (2012) Determination of radioactive elements and heavy metals in sediments and soil from domestic water sources in northern peninsular Malaysia. *Environ Monit Assess* 184(8):5043–5049. <https://doi.org/10.1007/s10661-011-2320-3>
33. Kılıç Ö, Belivermiş M, Topçuoğlu S, Çotuk Y, Coskun M, Çayır A, Kucer R (2008) Radioactivity concentrations and dose assessment in surface soil samples from east and south of Marmara region, Turkey. *Radiat Prot Dosim* 128(3):324–330. <https://doi.org/10.1093/rpd/ncm400>
34. Morton B, Blackmore G (2001) South China Sea. *Mar Pollut Bull* 42(12):1235–1263
35. Xu LQ, Liu XD, Sun LG, Yan H, Liu Y, Luo YH, Huang J (2011) Geochemical evidence for the development of coral island ecosystem in the Xisha Archipelago of South China Sea from four orthogenic sediment profiles. *Chem Geol* 286(3):135–145. <https://doi.org/10.1016/j.chemgeo.2011.04.015>
36. Zhao QH, Wang PX (1999) Progress in Quaternary paleoceanography of the South China Sea: a review. *Quat Sci* 06:481–501
37. Liu JG, Xiang R, Chen Z, Chen MH, Yan W, Zhang LL, Chen H (2013) Sources, transport and deposition of surface sediments from the South China Sea. *Deep Sea Res Part I Oceanogr Res Pap* 71:92–102. <https://doi.org/10.1016/j.dsr.2012.09.006>
38. Yan HM (2016) Sediments sources and transportation from the continental shelf of the Northern South China Sea. M.D. Dissertation. China University of Petroleum.
39. Ji C, Xu LQ, Zhang YH, Guo M, Kong DM (2020) A 1900-year record of marine productivity in the upwelling area of east continental shelf of Hainan Island, South China Sea. *Mar Geol Quat Geol* 40(05):97–106. <https://doi.org/10.16562/j.cnki.0256-1492.2019092502>
40. Ji C, Xu LQ, Zhang YH, Guo M, Kong DM (2019) A 1900-year record of mercury (Hg) from the east continental shelf of Hainan Island, South China Sea. *Geol J* 55(6):4469–4478. <https://doi.org/10.1002/gj.3678>
41. UNSCEAR (2000) Sources and effects of ionizing radiation, United Nations Scientific Committee on the Effects of Atomic Radiation (UNSCEAR) 2000 Report, Volume II: Report to the General Assembly, with Scientific Annexes—Effects. United Nations: 2000
42. Fu YJ, Song G, Chen DY, Feng YS (2011) Studies on  $^{238}\text{U}$ ,  $^{226}\text{Ra}$ ,  $^{232}\text{Th}$  and  $^{40}\text{K}$  levels of Topsoils in Pearl River Delta Zone. *J Anhui Agric Sci* 39(30):18582–18584. <https://doi.org/10.13989/j.cnki.0517-6611.2011.30.061>
43. Liu GS, Huang YP, Chen M, Qiu YS, Cai YH, Gao ZY (2001) Specific activity and distribution of natural radionuclides and  $^{137}\text{Cs}$  in surface sediments of the northeastern South China Sea. *Acta Oceanol Sin* 23(06):76–84. <https://doi.org/10.3321/j.issn:0253-4193.2001.06.008>
44. Zhao F, Wu MG, Zhou P, Li DM, Zhao L, Zheng YL, Cai WX, Fang HD, Huang CG (2015) Radionuclides in surface sediments from the Huangmaohai Estuary–Guanghai Bay and its adjacent sea area of the South China Sea. *J Trop Oceanogr* 34(04):77–82. <https://doi.org/10.3969/j.issn.1009-5470.2015.04.011>
45. Wang WX, Yang YX, Wang LM, Liu QC, Xia YF (2005) Studies on natural radioactivity of soil in Xiazhuang uranium ore field, Guangdong. *China Environ Sci* 25(01):120–123. <https://doi.org/10.1360/biodiv.050058>
46. Mo CL (2010) The study on the investigation and evaluation of natural radioactivity ecological environment in Guangdong Province and the countermeasure. M.D. Dissertation. South of China University of Technology Guangzhou, China.
47. Wang Z (2002) Natural radiation environment in China. *Int Congr Ser* 1225(2002):39–46. [https://doi.org/10.1016/S0531-5131\(01\)00548-9](https://doi.org/10.1016/S0531-5131(01)00548-9)
48. Lin WH, Feng Y, Yu KF, Lan WL, Mo ZN, Ning QY, Feng LL, He XW (2019) Radionuclide level status and ionizing radiation evaluation in marine sediment of Beibu Gulf. In: Science and technology annual meeting of Chinese society of environmental sciences, vol 8
49. Mao YY, Lin J, Huang DK, Yu T (2018) Radionuclides in the surface sediments along the coast of Bailong Peninsula in Beibu Gulf. *J Appl Oceanogr* 37(02):194–202
50. Ding MX, Liu GQ, Feng JP, Shi JS, Luo Q, Guo ZM (2017) Study on radionuclide concentrations in seawater and sediments from the Pearl River estuary, Dapeng Bay and Daya Bay. *Radiat Prot* 37(06):453–458
51. Ding MX, Liu GQ, Su LL, Feng JP, Shi JS, Luo Q (2017) Radionuclides in seawater and sediments from near-shore area of Shenzhen. *J Nucl Radiochem* 39(06):442–446
52. Liu GS, Huang YP, Chen M, Qiu YS (2001) Distribution features of radionuclides in surface sediments of Nansha sea areas.

- Mar Sci 25(8):1–5. <https://doi.org/10.3969/j.issn.1000-3096.2001.08.001>
53. Jia CX, Liu GS, Xu MQ, Huang YP, Zhang J (2003) Radionuclides and minerals in surface sediments of Jiaozhou Bay. *Oceanologia Et Limnologia Sinica* 34(05):490–498. <https://doi.org/10.11693/hyh200305004004>
  54. Chen JF, Liu GS, Huang YP (2005) Disequilibrium of natural decay series in sediments of intertidal mudflats of Xiamen. *J Oceanogr Taiwan Strait* 24(03):274–282. <https://doi.org/10.1360/gso50302>
  55. Li DM, Xu MQ, Liu GS, Li C, Xu WB (2005) The distribution of radionuclides in sediment cores from offshore area of Xinghua Bay. In: The 8th national symposium on isotope geochronology and isotope geochemistry, vol 4
  56. Zuo SH, Han ZY, Xie HL, Li HY, Huang YX (2019) Radionuclide content in surface sediments of Taiwan Sea area in Lianyungang. *Adm Tech Environ Monit* 31(6):42–45. <https://doi.org/10.19501/j.cnki.1006-2009.20191122.002>
  57. González-Fernández D, Garrido-Pérez MC, Casas-Ruiz M, Barbero L, Nebot-Sanz E (2012) Radiological risk assessment of naturally occurring radioactive materials in marine sediments and its application in industrialized coastal areas: Bay of Algeciras, Spain. *Environ Earth Sci* 66(4):1175–1181. <https://doi.org/10.1007/s12665-011-1325-0>
  58. Yii MW, Zaharudin A, Abdul-Kadir I (2009) Distribution of naturally occurring radionuclides activity concentration in East Malaysian marine sediment. *J Appl Radiat Isot* 67(4):630–635. <https://doi.org/10.1016/j.apradiso.2008.11.019>
  59. Singh S, Rani A, Rk M (2005)  $^{226}\text{Ra}$ ,  $^{232}\text{Th}$  and  $^{40}\text{K}$  analysis in soil samples from some areas of Punjab and Himachal Pradesh, India using gamma ray spectrometry. *Radiat Meas* 39(4):431–439. <https://doi.org/10.1016/j.radmeas.2004.09.003>
  60. Kurnaz A, Kucukomeroglu B, Keser R, Okumusoglu NT, Korkmaz F, Karahan G, Cevik U (2007) Determination of radioactivity levels and hazards of soil and sediment samples in Firtina Valley (Rize, Turkey). *Appl Radiat Isot* 65(11):1281–1289. <https://doi.org/10.1016/j.apradiso.2007.06.001>
  61. Yang WF, Chen M, Liu GS, Huang YP (2005) Distribution of radionuclides at surface sediments in Chukchi Shelf. *Mar Environ Sci* 24(02):32–35
  62. Tufail M (2012) Radium equivalent activity in the light of UNSCEAR report. *Environ Monit Assess* 184(9):5663–5667. <https://doi.org/10.1007/s10661-011-2370-6>
  63. Lin WH, Yu KF, Wang YH, Liu XM, Wang JJ, Ning QY, Li YH (2018) Extremely low radioactivity in marine sediment of coral reefs and its mechanism. *Chin Sci Bull* 63(21):2173–2183. <https://doi.org/10.1360/n972017-01101>
  64. Harb S (2008) Natural radioactivity and external gamma radiation exposure at the coastal Red Sea in Egypt. *Radiat Prot Dosim* 130(3):376–384. <https://doi.org/10.1093/rpd/ncn064>
  65. Beretke J, Mathew PJ (1985) Natural radioactivity of Australian building materials, industrial wastes and by-products. *Health Phys* 48(1):87–95. <https://doi.org/10.1097/00004032-198501000-00007>
  66. Ravisankar R, Chandramohan J, Chandrasekaran A, Prince Prakash Jebakumar J, Vijayalakshmi I, Vijayagopal P, Venkatraman B (2015) Assessments of radioactivity concentration of natural radionuclides and radiological hazard indices in sediment samples from the East coast of Tamilnadu, India with statistical approach. *Mar Pollut Bull* 97(1–2):419–430. <https://doi.org/10.1016/j.marpolbul.2015.05.058>
  67. Chandramohan J, Tholkappian M, Harikrishnan N, Ravisankar R (2015) The natural radioactivity measurements in coastal sediment samples along the East Coast of Tamilnadu using gamma spectrometry technique. In: Advanced materials and radiation physics (AMRP-2015) AIP Conf. Proc. 1675, 020049-1-020049-4, United States. <https://doi.org/10.1063/1.4929207>
  68. Abdi MR, Hassanzadeh S, Kamali M, Raji HR (2009)  $^{238}\text{U}$ ,  $^{232}\text{Th}$ ,  $^{40}\text{K}$  and  $^{137}\text{Cs}$  activity concentrations along the southern coast of the Caspian Sea, Iran. *Mar Pollut Bull* 58(5):658–662. <https://doi.org/10.1016/j.marpolbul.2009.01.009>
  69. Botwe BO, Schirone A, Delbono I, Barsanti M, Delfanti R, Kelderman P, Nyarko E, Lens PNL (2019) Radioactivity concentrations and their radiological significance in sediments of the Tema Harbour (Greater Accra, Ghana). *J Radiat Res Appl Sci* 10(1):63–71. <https://doi.org/10.1016/j.jrras.2016.12.002>
  70. Al-Absi E, Manasrah R, Wahsha M, Al-Makahleh M (2016) Radionuclides levels in marine sediment and seagrass in the northern Gulf of Aqaba, Red Sea. *Fresenius Environ Bull* 25(9):3461–3474
  71. Li SQ (1987) China's offshore radioactivity level. China Ocean Press, Beijing
  72. Wang JL, Du JZ, Zhang J (2012) Distribution of natural nuclides in moving mud and surface sediments of the Yangtze River Estuary and its adjacent sea areas and its dose evaluation. In: The 11th national symposium on nuclear chemistry and radiochemistry, vol 1
  73. Yu KN, Guan ZJ, Stokes MJ, Young ECM (1994) Natural and artificial radionuclides in seabed sediments of Hong Kong. *Nucl Geophys* 8(1):45–48
  74. Liu GS, Li DM, Yi Y, Liu SM, Bai J, Zhang J (2008) Radionuclide distribution in sediments and sedimentary rates in the Jiaozhou Bay. *Acta Geosci Sin* 29(6):769–777. <https://doi.org/10.3321/j.issn:1006-3021.2008.06.018>
  75. Alexander CR, Windom HL (1999) Quantification of natural backgrounds and anthropogenic contaminants in a pristine arctic environment: the Anadyr River Basin, Chukotka Peninsula, Russia. *Mar Pollut Bull* 38(4):276–284. [https://doi.org/10.1016/S0025-326X\(98\)90146-1](https://doi.org/10.1016/S0025-326X(98)90146-1)
  76. Powell BA, Hughes LD, Soreefan AM, Falta D, Wall M, DeVol TA (2007) Elevated concentrations of primordial radionuclides in sediments from the Reedy River and surrounding creeks in Simpsonville, South Carolina. *J Environ Radioact* 94(3):121–128. <https://doi.org/10.1016/j.jenvrad.2006.12.013>
  77. Yang YX, Wu XM, Jiang ZY, Wang WX, Lu JG, Lin J, Wang LM, Hsia YF (2005) Radioactivity concentrations in soils of the Xiashuang granite area, China. *Appl Radiat Isot* 63(2):255–259. <https://doi.org/10.1016/j.apradiso.2005.02.011>
  78. Akhtar N, Tufail M, Ashraf M, Mohsin Iqbal M (2005) Measurement of environmental radioactivity for estimation of radiation exposure from saline soil of Lahore, Pakistan. *Radiat Meas* 39(1):11–14. <https://doi.org/10.1016/j.radmeas.2004.02.016>
  79. Papaefthymiou HV, Chourdakis G, Vakalas J (2011) Natural radionuclides content and associated dose rates in fine-grained sediments from Patras-Rion sub-basins, Greece. *Radiat Prot Dosim* 143(1):117–124. <https://doi.org/10.1093/rpd/ncq345>
  80. Matiullah A, Ahad A, ur Rehman S, ur Rehman S, Faheem M (2004) Measurement of radioactivity in the soil of Bahawalpur division, Pakistan. *Radiat Prot Dosim* 112(3):443–447. <https://doi.org/10.1093/rpd/nch409>
  81. Al-Trabulsi HA, Khater AEM, Habbani FI (2011) Radioactivity levels and radiological hazard indices at the Saudi coastline of the Gulf of Aqaba. *Radiat Phys Chem* 80(3):343–348. <https://doi.org/10.1016/j.radphyschem.2010.09.002>
  82. Özmen SF, Cesur A, Boztosun I, Yavuz M (2014) Distribution of natural and anthropogenic radionuclides in beach sand samples from Mediterranean Coast of Turkey. *Radiat Phys Chem* 103:37–44. <https://doi.org/10.1016/j.radphyschem.2014.05.034>
  83. Zare MR, Mostajaboddavati M, Kamali M, Abdi MR, Mortazavi MS (2012)  $^{235}\text{U}$ ,  $^{238}\text{U}$ ,  $^{232}\text{Th}$ ,  $^{40}\text{K}$  and  $^{137}\text{Cs}$  activity concentrations in marine sediments along the northern coast of Oman Sea using high-resolution gamma-ray spectrometry. *Mar Pollut Bull*

- 64(9):1956–1961. <https://doi.org/10.1016/j.marpolbul.2012.05.005>
84. Kritsanuwat R, Sahoo SK, Fukushi M, Pangza K, Chanyotha S (2014) Radiological risk assessment of  $^{238}\text{U}$ ,  $^{232}\text{Th}$  and  $^{40}\text{K}$  in Thailand coastal sediments at selected areas proposed for nuclear power plant sites. *J Radioanal Nucl Chem* 303(1):325–334. <https://doi.org/10.1007/s10967-014-3376-7>
85. Agbalagba EO, Onoja RA (2011) Evaluation of natural radioactivity in soil, sediment and water samples of Niger Delta (Biseni) flood plain lakes, Nigeria. *J Environ Radioact* 102(7):667–671. <https://doi.org/10.1016/j.jenvrad.2011.03.002>
86. Korkulu Z, Özkan N (2013) Determination of natural radioactivity levels of beach sand samples in the black sea coast of Kocaeli (Turkey). *Radiat Phys Chem* 88:27–31. <https://doi.org/10.1016/j.radphyschem.2013.03.022>
87. Yii MW, Wan Mahmood Z, Ahmad Z, Md. Jaffary NA, Ishak K (2011) NORM activity concentration in sediment cores from the Peninsular Malaysia East Coast Exclusive Economic Zone. *J Radioanal Nucl Chem* 289(3):653–661. <https://doi.org/10.1007/s10967-010-0928-3>
88. Venturini L, Nisti MB (1997) Natural radioactivity of some Brazilian building materials. *Radiat Prot Dosim* 71(3):227–229. <https://doi.org/10.1093/oxfordjournals.rpd.a032058>
89. Yang G, Lu XW, Zhao CF, Li N (2013) Natural radioactivity in building materials used in Changzhi, China. *Radiat Prot Dosim* 155(4):512–516. <https://doi.org/10.1093/rpd/nct018>

**Publisher's Note** Springer Nature remains neutral with regard to jurisdictional claims in published maps and institutional affiliations.